

***In situ* ESR study to detect the diffusion of free H and creation of dangling bonds in hydrogenated amorphous silicon**

U. K. Das,* T. Yasuda, and S. Yamasaki

Joint Research Center for Atom Technology, 1-1-4 Higashi, Tsukuba, Ibaraki 305 0046, Japan

(Received 23 October 2000; published 6 June 2001)

In situ electron spin resonance (ESR) was studied during exposure of hydrogenated amorphous silicon (*a*-Si:H) films to atomic hydrogen (H) generated by a remote plasma. A high diffusion coefficient of free atomic H ($> 10^{-10} \text{ cm}^2 \text{ s}^{-1}$) is observed in *a*-Si:H films at the very initial stage of H treatment. The H creates additional dangling bonds ($\sim 10^{13} \text{ cm}^{-2}$) during in-diffusion. The diffusion mechanism of such free H is a self-limiting process. The dangling bonds created at the very initial stage of H exposure act as the trapping sites for the impinging H atoms. Consequently, the effective diffusion coefficient (D_{eff}) reduces with H treatment time. The D_{eff} for plasma in-diffusion of H with a relatively wide time span reported in literature is considered to be the resultant of the diffusion coefficient of free H and the bonded H. The characteristic depth of dangling-bond distribution decreases with increasing H treatment temperature. The activated rate constants of db creation reactions dominate over the activated free-H diffusion to determine the distribution of additional dangling bonds at different treatment temperatures.

DOI: 10.1103/PhysRevB.63.245204

PACS number(s): 61.43.Dq, 52.77.Bn, 76.30.-v, 66.30.Ny

I. INTRODUCTION

Hydrogen and its isotopes are known to play important roles in modifying the optical, electrical, and structural properties of various semiconductors. In many cases, hydrogen appears as an undesirable contamination in crystalline semiconductors (Si, GaAs, etc.) and passivates the shallow acceptors and donors.¹⁻³ Such a passivation of the intended electrical activity of dopants is detrimental to the performance of devices based on these semiconductors. On the other hand, hydrogen and its isotopes are intentionally used to passivate the electrical activity of many deep defects. Some of the beneficial properties of hydrogen or deuterium (H/D) are the passivation of Si/SiO₂ interface defects to improve the quality of metal-oxide-semiconductor (MOS) transistors,^{4,5} passivation of grain boundary defects in polycrystalline Si for improving its electrical properties,⁶ and the passivation of Si dangling bonds (db's) in amorphous silicon (*a*-Si).⁷⁻⁹ Owing to the large reduction of deep db's ($> 10^3$ orders of magnitude) in hydrogenated amorphous silicon (*a*-Si:H), the materials immediately found many applications in thin-film transistors, solar cells, image sensors, and many other optoelectronic devices. Thus the various effects of hydrogen on semiconductors have a profound impact on devices. Therefore, studies on the interaction of atomic hydrogen with Si and the dynamic changes of Si matrices are of relevance to various Si technologies. In this work we confine our discussions to the role of hydrogen in *a*-Si:H thin films.

The saturation of host db's in amorphous Si, amorphous Ge, and related alloys by H enables such hydrogenated materials to contain 10–20 at. % bonded hydrogen and less than 10^{16} cm^{-3} db defects in the films.¹⁰⁻¹² It was soon realized that H not only passivates the db's in *a*-Si:H but also may completely change the macroscopic structures of the materials.¹³ Excessive admixture of hydrogen with SiH₄ in a plasma-enhanced chemical-vapor deposition (CVD) system results in the ordering of an amorphous network and the

formation of microcrystallites in the amorphous matrix.^{14,15} Alternate deposition of *a*-Si:H films and the H plasma treatment (commonly known as hydrogen “chemical annealing”) changes the *a*-Si:H film structure in a wide range.¹⁶⁻¹⁹ The optical gap of *a*-Si:H films (in the range 1.7–2.1 eV) and the formation of crystallinity can be controlled only by varying the ratio of H plasma treatment time to film deposition time.¹⁹ So all these experimental results suggest the crucial role of H in tailoring the structure of silicon-hydrogen alloy films. On the other hand, H is suggested to be responsible for the creation of metastable defects under light illumination or current injection. The motion of H is suspected to cause the generation of light or carrier-induced defects in some models.²⁰⁻²³ The diffusion of hydrogen in the *a*-Si:H films may also anneal out the metastable defects at a temperature higher than 150 °C. The region over which hydrogen will have an influence and cause all the above-mentioned phenomena is obviously related to its diffusion depth in the materials. Therefore, much research has focused on the state of hydrogen and its diffusion process in *a*-Si:H films.

The state and amount of bonded hydrogen in *a*-Si:H films is often quantitatively estimated by the nuclear magnetic resonance (NMR) measurement,²⁴ infrared-absorption (IR) spectroscopy,²⁵⁻²⁸ and hydrogen effusion measurements.²⁹⁻³¹ On the other hand, the diffusion of hydrogen in *a*-Si:H films is generally studied by secondary-ion mass spectroscopy (SIMS).³¹⁻³⁴ The concentration profile of hydrogen/deuterium in multilayers of *a*-Si:D/*a*-Si:H can be obtained by studying the SIMS depth profile. The SIMS depth profile for the thermally annealed *a*-Si:D/*a*-Si:H layer shows that the total concentration of D plus H remains almost the same, whereas their individual concentrations (c) vary in the *a*-Si:H/*a*-Si:D layer with the distance (x) and time (t), according to

$$c = c_0 \operatorname{erfc} \left\{ \frac{x}{2(D_{\text{eff}}t)^{1/2}} \right\}, \quad (1)$$

where c_0 and D_{eff} are the initial concentration of D/H in the a -Si:D/ a -Si:H layer and the diffusion coefficient of D/H, respectively. Their respective bond-switching processes can describe the diffusion mechanism of D/H in such cases. However, this layer diffusion process of H(D), which originates internally from the solid, does not adequately explain the diffusion of mobile H(D) when it is introduced from a plasma at the surface. In fact, the plasma deuteration of a -Si:H films results in a several orders of magnitude higher diffusion coefficient in the low-temperature range ($<400^\circ\text{C}$) with a significantly lower diffusion barrier.^{33,34} Several attempts have been made to observe the effect of hydrogen or deuterium plasma treatment on a -Si:H films in real time by *in situ* ellipsometry and *in situ* IR studies. The *in situ* ellipsometry results suggest that the diffusion coefficient of atomic hydrogen generated by a filament heated in H_2 gas may be much higher than $3 \times 10^{-15} \text{ cm}^2 \text{ s}^{-1}$ at 250°C .³⁵ The *in situ* IR studies show the formation of a Si-H plateletlike structure during H exposure in various a -Si:H films.³⁶

The mechanism of H incorporation and its influence on the microscopic defects of a -Si:H films remains unknown. The kinetics of the creation, termination, and annihilation of the db during a -Si:H film growth and H_2 plasma treatment have recently been successfully realized by *in situ* electron spin resonance (ESR) studies using the remote plasma microwave CVD method.³⁷⁻⁴⁰ Our earlier experiments showed that hydrogen creates additional db's in a -Si:H films during H exposure.³⁹ Moreover, it was observed that these excess db's were created not only at the top surface but also at some regions below the surface, unlike the Ar plasma treatment on a -Si:H films.³⁹ Recently, we found an unusually high diffusion coefficient of H in a -Si:H films at the very initial stage of H_2 plasma treatment of a -Si:H films.⁴¹ In this paper we report in detail on the depth of the distribution of additional db's [$\Delta n_s(x, t)$, where x is the depth of the a -Si:H film and t is the H treatment time] due to H exposure, and the effect of H treatment temperature on the distribution of Δn_s . The D plasma treatment on a -Si:H films and the subsequent SIMS depth profile for D has been recorded to understand the difference between *in situ* ESR and previously reported results. The kinetics of the various reactions of H with the Si network are discussed based on the experimental results.

II. EXPERIMENTAL DETAILS

A remote plasma microwave (2.45 GHz) CVD method was used to deposit the a -Si:H films inside an X-band (9 GHz) ESR cavity. Hydrogen plasma was generated above the ESR cavity in a T -shaped high-purity vitreous silica (HPVS) tube using microwave (MW) power. The atomic H formed in the plasma was admitted into the ESR cavity through the T -shaped tube (outer diameter of 6 mm). The source gas silane (SiH_4) was introduced through another coaxial HPVS tube with a larger diameter (inner diameter of 8 mm) and reacted with atomic H ($\text{H} + \text{SiH}_4 \rightarrow \text{SiH}_3 + \text{H}_2$) in the ESR cavity for a -Si:H deposition. The flow of SiH_4 was stopped for H treatment of the deposited a -Si:H film. The experimental setup has been described elsewhere.^{37,38} A flow of hot N_2 gas was used to raise the substrate temperature

(wall temperature of the 8-mm HPVS tube) from room temperature up to 200°C . A cylindrical ESR cavity with an inner diameter of 20 mm was used to allow enough space for the N_2 gas to flow. The typical experimental conditions were a H_2 flow rate of 100 SCCM and a SiH_4 flow rate of 10 SCCM for deposition (where SCCM denotes cubic centimeter per minute at STP). A H_2 flow rate of 100 SCCM was used for H treatment. Other parameters were the microwave power for sustaining H_2 plasma of 50 W and the pressure of ~ 1.5 Torr. The flux of atomic hydrogen during H treatment under the above plasma conditions was estimated to be $\sim 3 \times 10^{16} \text{ cm}^{-2} \text{ s}^{-1}$ from the measurements of gas-phase ESR. The flux of atomic H to the film surface can be varied by changing the flow rate of H_2 and the microwave power. In our present experimental setup, the flux of H can be varied by about one order of magnitude. The *in situ* ESR measurements were performed during deposition and H treatment at different temperatures using a BRUKER ESP 300E spectrometer. To obtain the time evolution of Si db's, the magnetic field for ESR was set at the peak position of the first derivative spectrum due to neutral Si db's ($g = 2.0055$).⁴²

To realize the spatial distribution of db's in a -Si:H films during H treatment, we performed a thickness dependence study of H treatment at different temperatures. If the db's are created only at the film surface, the resulting additional db's [i.e., the total db's created in the film of thickness d due to H exposure; $\Delta N_s = \int_0^d \Delta n_s(x, \infty) dx$, where $\Delta n_s(x, \infty)$ denotes the value of the equilibrated Δn_s at film depth x] will be independent of film thickness. Otherwise, for a deeper spatial distribution of the db's, ΔN_s should increase with the film thickness. H plasma treatment for 3 min was repeated after each deposition (namely, at each film thickness). We did not observe any significant etching of a -Si:H film during 3 min of H treatment under our plasma conditions. The ESR intensities were averaged over 1024 data accumulated during 84 s to increase the signal-to-noise ratio. The ΔN_s at each film thickness were estimated from the ESR intensities during H treatment, which were performed after 15 min of each deposition. Also, we performed separate deposition and subsequent H treatment to check for any influence of the repeated deposition and H treatment on the ΔN_s value, but the ΔN_s value was almost the same in both cases. For the SIMS depth profile study, we deposited an a -Si:H film (thickness ~ 165 nm) at room temperature (RT). The film deposited at the same run was cut into four pieces. Three of the pieces were subsequently treated by D_2 plasma at RT for 10, 100, and 1000 s, respectively, while the remaining piece was untreated and used as a reference sample. The SIMS depth profile of deuterium was recorded using Cs^+ as a sputtered beam with a width of $140 \times 224 \text{ mm}^2$ and a sputtering rate of 0.4 nm/s.

III. RESULTS

A typical time evolution of ESR intensity during a -Si:H deposition and its subsequent exposure to a flux of H ($\Phi_{\text{H}} = 3 \times 10^{16} \text{ cm}^{-2} \text{ s}^{-1}$) at 150°C is shown in Fig. 1. In this case, the H treatment was performed after a long time (~ 1500 min) of deposition. The deposition temperature (T_d)

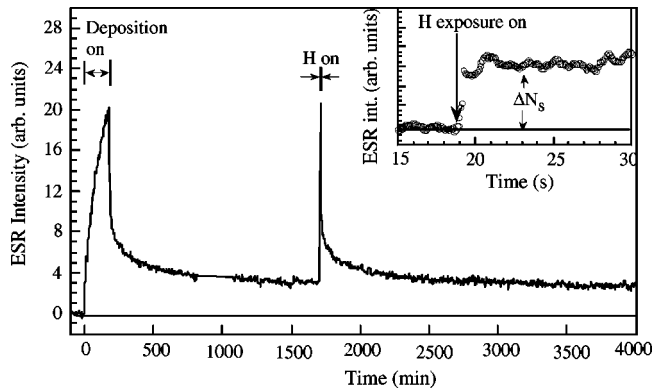


FIG. 1. Time evolution of the ESR intensity during a -Si:H film deposition and the subsequent H treatment of the deposited film at 150°C . The inset shows the time evolution of the ESR intensity at the very initial stage of the H treatment.

was the same as the H treatment temperature (T_p). The ESR intensity rises sharply at the initial stage of deposition, which may be attributed to the formation of a film surface with high db's. After the formation of the film surface, the ESR intensity (in other words, the number of db's) increases continuously due to the growth of the bulk film. The ESR intensity decays with time after stopping the film deposition due to the structural relaxation. The details of the deposition processes and the mechanism of the db decay after deposition will be discussed elsewhere. The ESR intensity rises sharply as soon as the film is exposed to atomic H. The decrease of the ESR intensity after H treatment is quite similar to the decay of the ESR intensity observed after film growth (Fig. 1). The inset of Fig. 1 shows the time evolution of the Si db signal at the initial stage of H exposure. A rapid increase of ESR intensity (with time constant less than 1 s) followed by the saturation of the ESR signal is observed during H exposure to the a -Si:H film. We estimate the amount of additional db's, ΔN_s , due to H exposure, which were performed after 15 min of deposition, by subtracting the ESR signal during H exposure to the ESR signal before H treatment, as shown in the inset of Fig. 1.

To observe the dependence of ΔN_s on the flux of H, we deposited a film of thickness ~ 400 nm at 150°C and treated it by different incident flux of H. Figure 2 shows the variation of ΔN_s with Φ_H . Interestingly, we observed that the

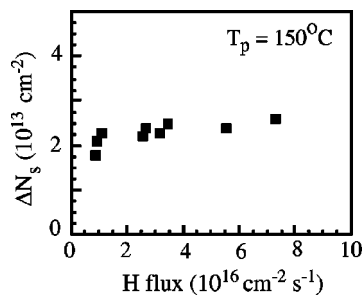


FIG. 2. Dependence of additional db's (ΔN_s) that are created during H treatment at 150°C on the incident flux of atomic H. The flux of H was varied by changing the MW power and the flow rate of H_2 .

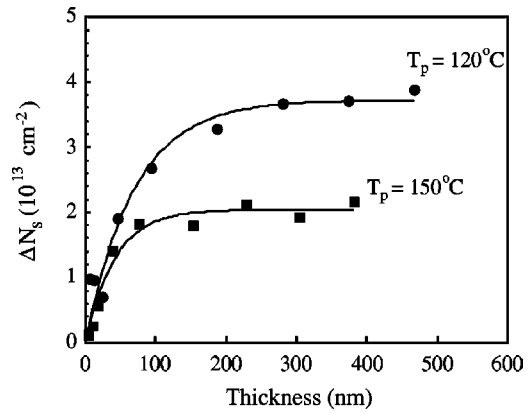


FIG. 3. Variation of total additional db's (ΔN_s) created in the a -Si:H films due to H exposure as a function of film thickness at treatment temperatures of 120°C and 150°C . Note that the deposition temperature was the same as the treatment temperature.

value of ΔN_s is almost independent of Φ_H in the range of $8 \times 10^{15} \text{ cm}^{-2} \text{ s}^{-1}$ to $7 \times 10^{16} \text{ cm}^{-2} \text{ s}^{-1}$.

Figure 3 shows the variation of ΔN_s as a function of film thickness for the a -Si:H films treated at 120°C and 150°C . The incident flux of atomic H was $3 \times 10^{16} \text{ cm}^{-2} \text{ s}^{-1}$. The figure shows that ΔN_s increases up to a film thickness of ~ 100 nm and remains constant for the thicker films. Thus the thickness dependence of ΔN_s suggests that the impinging H on the film surface can diffuse into the bulk of the film and indeed create additional db's. It is worth mentioning here that we did not observe ΔN_s at temperatures below 80°C in our present experimental conditions. Failure to observe ΔN_s at lower temperatures ($< 80^\circ\text{C}$) might be due to the following reason. The relaxation of the db's after deposition becomes slower at lower temperature.⁴⁰ Therefore the large number of db's, which remain even after 15 min from the deposition-off time, masks the creation of additional db's due to H exposure.

In all the experiments mentioned above, the substrate temperatures during film deposition (T_d) and during H treatment (T_p) were the same. Therefore, the different amount and spatial extent of ΔN_s at temperatures of 120°C and 150°C (Fig. 3) may be argued to be an effect of a different film structure caused from the different T_d and not an effect of T_p . To clarify the effect of the film structure on the ΔN_s distribution, we performed the film deposition and H treatment at different temperatures. In one case, we deposited a film at 200°C (T_d) and treated it by H at 100°C (T_p). In another case, the film was deposited at 150°C and treated at 100°C . Figure 4(a) compares the data of the films with $T_d = 200^\circ\text{C}$, $T_p = 100^\circ\text{C}$, and the data of the films with the same temperature of deposition and H treatment (viz., T_d , $T_p = 200^\circ\text{C}$, and T_d , $T_p = 100^\circ\text{C}$.) On the other hand, Fig. 4(b) compares the films with $T_d = 150^\circ\text{C}$, $T_p = 100^\circ\text{C}$ and the films with T_d , $T_p = 150^\circ\text{C}$ and T_d , $T_p = 100^\circ\text{C}$. Figure 4(a) shows that the data of $T_d = 200^\circ\text{C}$, $T_p = 100^\circ\text{C}$ (open circles) closely resemble the data of $T_d = 100^\circ\text{C}$, $T_p = 100^\circ\text{C}$ (filled circles). Figure 4(b) shows the resemblance of $T_d = 150^\circ\text{C}$, $T_p = 100^\circ\text{C}$ (open circles) with the data of $T_d = 100^\circ\text{C}$, $T_p = 100^\circ\text{C}$ (filled circles). Thus Figs. 4 sug-

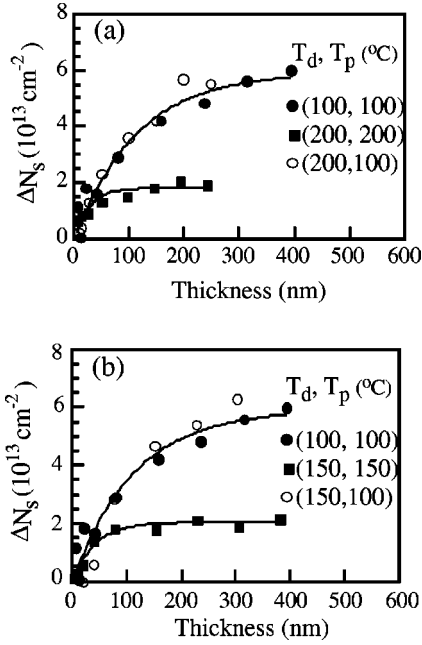


FIG. 4. Comparison of the thickness dependence of ΔN_s for different deposition and treatment temperatures. (a) Deposition temperature (T_d) of 100 °C, H treatment temperature (T_p) of 100 °C (filled circles); T_d of 200 °C, T_p of 200 °C (filled squares); T_d of 200 °C, T_p of 100 °C (open circles). (b) T_d of 100 °C, T_p of 100 °C (filled circles); T_d of 150 °C, T_p of 150 °C (filled squares); T_d of 150 °C, T_p of 100 °C (open circles). The solid lines are the fits of the data points to Eq. (10).

gest that the amount and the spatial distribution of Δn_s mainly depend on the H treatment temperature (T_p). Therefore, any possible change in film structure due to different T_d has a negligible effect on ΔN_s in the temperature range of 80 °C–200 °C.

Until now, we have described the results of *in situ* ESR during H treatment which illustrates the evolution of Si dangling bonds due to the in-diffusion of free H into the *a*-Si:H films. The amount of bonded hydrogen would also be expected to increase in the film during H treatment. To observe the change of the amount of hydrogen in the film due to in-diffusion, we performed a D_2 plasma treatment on *a*-Si:H films and observed the SIMS depth profile for deuterium. Figure 5 shows the SIMS depth profile of D in the *a*-Si:H film deposited and treated by D_2 plasma at RT for 10, 100, and 1000 s. The depth profile of D for an untreated film has also been included in the figure as a reference, which exhibits the background concentration of deuterium in our *a*-Si:H films is $\sim 10^{18} \text{ cm}^{-3}$. Even for the 10 s D_2 plasma treatment, the film contains greater than 10^{20} cm^{-3} D at the film surface and deuterium is detected (greater than 10^{18} cm^{-3}) at a film depth of ~ 12 nm. The concentration of D atoms at the film surface increases to $\sim 3 \times 10^{21} \text{ cm}^{-3}$ for 1000 s treatment, while the distribution of D atoms extends up to a film depth of ~ 20 nm. Therefore, it is evident from Fig. 5 that the total concentration of D in the film increases with the D_2 plasma treatment time. Therefore, the concentration of in-diffusing D does not attain a steady state within a short treatment time,

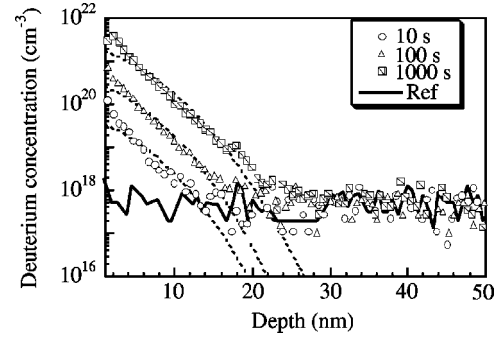


FIG. 5. The deuterium (D) depth profiles as seen by secondary-ion mass spectroscopy (SIMS) in the *a*-Si:H films treated by D_2 plasma at RT for 10, 100, and 1000 s. The D depth profile for an untreated *a*-Si:H film is also shown for reference (solid line).

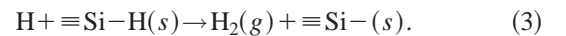
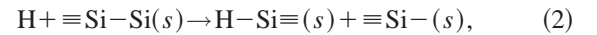
unlike the generation of additional db's due to in-diffusion of free H (inset of Fig. 1).

The concentration profile of D with film depth does not exactly follow Eq. (1) for our short-time deuterium plasma treatment case. The depth profiles rather decrease exponentially with the film depth from the top surface (decays almost linearly in the semilogarithmic plot as shown in Fig. 5). However, a deliberate attempt to fit the SIMS data to Eq. (1) is shown by dashed lines in Fig. 5. From the fitting, the values of the effective H diffusion coefficient (D_{eff}) are roughly estimated. The effective diffusion coefficients of deuterium for 10, 100, and 1000 s plasma treatment appear to be $1.4 \times 10^{-14} \text{ cm}^2 \text{ s}^{-1}$, $1.4 \times 10^{-15} \text{ cm}^2 \text{ s}^{-1}$, and $1.7 \times 10^{-16} \text{ cm}^2 \text{ s}^{-1}$, respectively. Therefore, it appears from the SIMS depth profile that the amount of incorporated D in the film and the diffusion coefficient, D_{eff} , both strongly depend on the plasma treatment time.

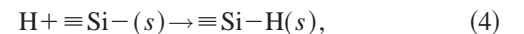
IV. FREE H DIFFUSION AND CREATION OF DANGLING BONDS IN *a*-Si:H

The *in situ* ESR studies during H treatment of *a*-Si:H films suggest that the additional db's are created not only on the film surface but also in the bulk region of the films (Fig. 3). Primarily, a H atom can create a db in *a*-Si:H films by a number of competitive processes.

(i) The creation of dangling bonds,

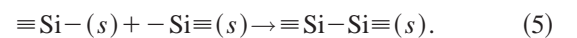


(ii) The termination of dangling bonds,

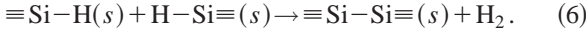


where g , s , H, and $\equiv \text{Si} - (s)$ denote the gas phase, solid phase, free hydrogen, and a Si db, respectively.

(iii) The annihilation of two nearby db's mainly by thermal reconstruction. Although it is not directly related to the interaction of H, it contributes to ΔN_s ,



(iv) The effusion of molecular H_2 from two nearby Si-H. Although it does not control the evolution of the db, it is an important process for stabilizing the a -Si:H matrix,⁴³



A net increase in the ESR intensity during H treatment (inset of Fig. 1) suggests that processes (2) and/or (3) dominate over processes (4) and (5) during H exposure of the a -Si:H films. The reverse reaction of Eqs. (3) and (4) may be argued to be significant to terminate or create db's. The reverse reaction of Eq. (3) suggests the termination of Si db's by a H_2 molecule to form an atomic H and an Si-H bond. However, it is well known that molecular H_2 hardly reacts with Si db's in a Si (111) 7×7 surface unlike the case of reactive atomic H. Actually, we observed much less reactivity of H_2 with the Si db's (adatom db's) on the crystalline Si(111) 7×7 surface in our ultrahigh vacuum (UHV) ESR during molecular H_2 exposure. Therefore, we think that the reverse reaction of Eq. (3) will not play an important role in determining ΔN_s during H treatment on a -Si:H films. On the other hand, the reverse reaction of Eq. (4) implies the thermal desorption of hydrogen from a Si-H bond to create a db. However, we believe that the desorption of H is negligible for our temperature range ($\leq 200^\circ\text{C}$) of studies and on the time scale of our interest.

The relaxation processes (5) and (6) may occur even in the absence of the flux of H, i.e., after stopping the H treatment. The processes are strongly dependent on T_p and their rates increase with T_p as observed after switching off the plasma.⁴⁰ Process (6) should have a large influence on equilibrating the H concentration in the film during H treatment and on determining the amount of bonded H in the film after H treatment.

The spatiotemporal variation of additional db's [$\Delta n_s(x, t)$] due to the in-diffusion of H can be described as follows. The densities of $\equiv \text{Si}-\text{Si}\equiv$ and $\equiv \text{Si}-\text{H}$ are considerably larger than the concentration of free H (H_f) and Si db's. Therefore, these densities are considered as constants. The H_f diminishes as H diffuses from the surface into the bulk due to the reactions (2)–(4). The rate of change of $H_f(x, t)$ and the variation of $\Delta n_s(x, t)$ due to the reactions (2)–(5) can be simultaneously expressed as

$$\frac{\partial H_f}{\partial t} = D_f \frac{\partial^2 H_f}{\partial x^2} - H_f [k_{\text{ins}} N_{\text{Si-Si}} + k_{\text{abs}} N_{\text{Si-H}}] - H_f k_t \Delta n_s \quad (7)$$

and

$$\frac{\partial \Delta n_s}{\partial t} = H_f [k_{\text{ins}} N_{\text{Si-Si}} + k_{\text{abs}} N_{\text{Si-H}} - k_t \Delta n_s] - 2k_a (\Delta n_s)^2, \quad (8)$$

where k_{ins} , k_{abs} , k_t , and k_a are the reaction rates for the db creation by the ‘‘insertion’’ of H into Si-Si bonds [reaction (2)], the db creation by ‘‘abstraction’’ of H from Si-H bonds [reaction (3)], the db termination [reaction (4)], and the db annihilation [reaction (5)], respectively. The $N_{\text{Si-Si}}$ and $N_{\text{Si-H}}$ are the concentrations of $\equiv \text{Si}-\text{Si}\equiv$ and $\equiv \text{Si}-\text{H}$, respectively.

We tentatively assume that the square term of Eq. (8) describes the annihilation of two db's due to thermal reconstruction. The dominating terms in Eq. (7) and (8) will be determined by the reaction rate constants and the local densities of the reacting species. At steady state, $\partial H_f / \partial t = \partial \Delta n_s / \partial t = 0$. We categorize the following two regions.

Region I (near the vicinity of film surface): when $H_f(x)$ is large, the reaction rates of the db creation and termination [reactions (2)–(4)] are large and therefore the annihilation of two nearby db's will be negligible. In such a case, Δn_s will be independent of H_f . From Eq. (8) we get

$$\Delta n_s = \frac{k_1 N_{\text{Si-Si}} + k_2 N_{\text{Si-H}}}{k_3}. \quad (9)$$

Therefore, Δn_s will increase linearly with the depth of the film (x) in the vicinity of film surface (low- x region), and H_f will diminish exponentially from the surface [from Eq. (7)].

Region II (at a finite depth of the film): when the db creation and termination term in Eq. (8) becomes comparable to the db annihilation term, the Δn_s distribution appears to be much more complicated. We assume that the value of H_f reduces significantly and the annihilation rate becomes dominant over the termination term [reaction (5) dominates over reaction (4)] to make the steady state between the db creation and the db annihilation. Then Δn_s will be proportional to the square root of H_f , which decays exponentially with the film thickness (d). Reasonable fits of the experimental data are obtained (solid lines in Figs. 3 and 4) using

$$\Delta N_s = (\Delta N_s)_{\text{sat}} \left[1 - \exp\left(-\frac{d}{\lambda}\right) \right], \quad (10)$$

where $(\Delta N_s)_{\text{sat}}$ is a constant that depends on T_p and λ is the characteristic depth of the Δn_s distribution. Note that the characteristic diffusion depth of H_f will be $\lambda/2$, since Δn_s is proportional to the square root of H_f . The expression for λ can be approximated from Eqs. (7) and (8),

$$\lambda = 2 \sqrt{\frac{D_f}{k_1 N_{\text{Si-Si}} + k_2 N_{\text{Si-H}}}}. \quad (11)$$

The values of λ are estimated from the fitting and plotted as a function of T_p in Fig. 6. The values of λ are very sensitive to T_p , which reduce with increasing H treatment temperature (Fig. 6). Thus, from Eq. (11) and Fig. 6 we conclude that the activation energy of either or both of k_{ins} and k_{abs} is larger than the activation energy of the free H diffusion coefficient (D_f). The denominator term of Eq. (11) is denoted by the average rate constants for db creation [given by reactions (2) and (3)] times the average density of the a -Si:H network ($k_c \times N_m$) for the sake of simplicity. We estimated the difference of activation energies for the rate constants of the db creation (k_c) and for the free H diffusion coefficient (D_f) using Eq. (11). The inset of Fig. 6 shows the variation of $1/\lambda^2$ as a function of $1000/T_p$. The fitting of the curve to an exponential function gives an estimate of $(\Delta E_k - \Delta E_D)$ as ~ 0.4 eV, where ΔE_k and ΔE_D are the activation energy for k_c and D_f , respectively.

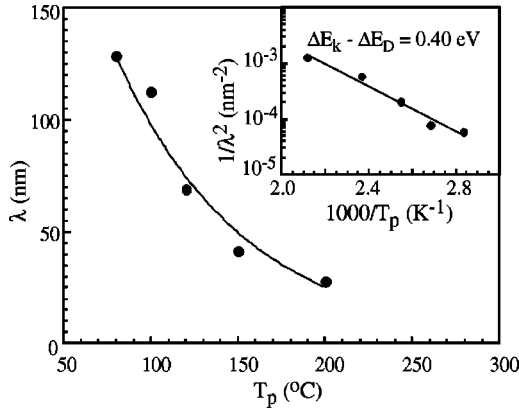


FIG. 6. Variation of the characteristic depth of the db distribution (λ) as a function of treatment temperature (T_p). The inset shows the Arrhenius plot for $1/\lambda^2$. The activation energy is the resultant of the activation energy for the db creation (ΔE_k) and the activation energy of the free H diffusion coefficient (ΔE_D).

V. DISCUSSION

In this work we recorded the ESR signal (presumably, the isolated Si dangling bonds) during H exposure to *a*-Si:H films and we attempted to discuss the diffusion coefficient of free H. The creation of some extra dangling bonds, $\sim 10^{13} \text{ cm}^{-2}$ (referred to as additional dangling bonds in this paper) during H exposure, is evident from our result. After stopping the H treatment, the db density in the films reduces due to the db annihilation given by reaction (5). Also the reaction (6), i.e., the effusion of hydrogen from the film, takes place after H treatment to determine the bonded H content.⁴³

The additional db's are created within a very short time (with a time constant less than 1 s; see the inset of Fig. 1) due to the in-diffusion of atomic H and its reaction with the *a*-Si:H network [reactions (2)–(5)]. The value of ΔN_s for a fixed film thickness is almost independent of the incident flux of H (Φ_H), as predicted from Eq. (9) and shown in Fig. 2. However, the time evolution of ΔN_s (hence the time constant for the ΔN_s creation) should depend on Φ_H [Eq. (8)].

The time constant for the evolution of ΔN_s is too small (possibly, much less than 1 s) to be resolved in our present experimental conditions and the time resolution of the ESR setup.

The thickness dependence of ΔN_s (Fig. 3) suggests that H diffuses to some depth (~ 100 nm) of the *a*-Si:H film and results in the additional db's (with the time constant less than 1 s). Therefore, considering the fast saturation of db's (the time constant is less than 1 s) during H treatment (the inset of Fig. 1) and the ΔN_s distribution of ~ 100 nm (Fig. 3), the diffusion coefficient of free H (D_f) appears to be larger than $10^{-10} \text{ cm}^2 \text{ s}^{-1}$ [$L = (D_f t)^{1/2}$, where L is the diffusion length and t is the diffusing time]. This result is in contrast with the usual activated type of H diffusion in *a*-Si:H films observed by thermal/plasma treatment and SIMS measurements.^{31–34}

Table I shows typical values of the effective H diffusion coefficient (D_{eff}) in *c*-Si and *a*-Si:H materials reported in the literature. Most of the earlier diffusion experiments were done at much higher temperatures (>200 °C) compared to the present study. Therefore, the values of D_{eff} shown in Table I are extrapolated to 200 °C for comparison. The coefficient for interdiffusion of H and D in a layered hydrogenated and deuterated *a*-Si is very low ($\sim 10^{-19} \text{ cm}^2 \text{ s}^{-1}$).^{32,45,46} For the plasma hydrogenation of *a*-Si:H films, D_{eff} increases by several orders of magnitude with a subsequent decrease in the diffusion activation energy.^{31,33,34} Beyer *et al.* observed a value of $D_{\text{eff}} \sim 10^{-15} \text{ cm}^2 \text{ s}^{-1}$ in *a*-Si:H films after 2 h of deuterium plasma treatment at 250 °C with a diffusion activation energy of 0.77 eV at temperatures less than 400 °C.³⁴ Abeles *et al.* observed plasma in-diffusion activation energy for deuterium of less than 1 eV with diffusion coefficient of $10^{-14} \text{ cm}^2 \text{ s}^{-1}$ at 160 °C.⁴⁷ An *et al.* suggested from their *in situ* ellipsometry studies during hot filament generated atomic H treatment on *a*-Si:H films that D_{eff} may be higher than $4 \times 10^{-14} \text{ cm}^2 \text{ s}^{-1}$.³⁵ From all these prior reports, it is suggested that the value of D_{eff} for plasma in-diffusion is much larger than that for layer diffusion. Also a range of D_{eff} ($>10^{-14} - 10^{-16} \text{ cm}^2 \text{ s}^{-1}$) for plasma in-diffusion was conjectured from various types and duration of experiments

TABLE I. Diffusion coefficients of hydrogen in *c*-Si and *a*-Si:H films measured by various techniques.

Material	Measurement technique	Diffusion coefficient ($\text{cm}^2 \text{ s}^{-1}$)	Refs.
<i>c</i> -Si	Mass spectrographic detection of hydrogen	$\sim 7 \times 10^{-8}$ (extrapolated to 200 °C)	44
<i>a</i> -Si:H	Interdiffusion of H and D by SIMS in layered structure of <i>a</i> -Si:H/ <i>a</i> -Si:D	$\sim 6 \times 10^{-19}$ (extrapolated to 200 °C)	32, 35, 46
<i>a</i> -Si:H	D plasma treatment on <i>a</i> -Si:H and subsequent SIMS depth profile study	$10^{-15} - 10^{-16}$ (extrapolated to 200 °C)	33, 34
<i>a</i> -Si:H	D plasma treatment on <i>a</i> -Si:H and SIMS depth profile study	$\sim 1 \times 10^{-14}$ at 160 °C	47
<i>a</i> -Si:H	Diffusion coefficient of mobile H studied by <i>in situ</i> ellipsometry	$> 4 \times 10^{-14}$ at 250 °C	35
<i>a</i> -Si:H	Diffusion coefficient of free H speculated from theoretical model	$\sim 10^{-6}$ at 200 °C	48

(Table I). The activation energy for such plasma in-diffusion of H varies in a wide range from 0.2 to 0.8 eV.^{31,33,34,49,50}

It is generally observed that “post hydrogenation” of *a*-Si:H films often increases the bonded H content in the film and changes the film structure significantly. Therefore, the deeper Δn_s distribution (~ 100 nm) observed in this study may be argued to be due to large modification of the film structure during H treatment. The *a*-Si:H film surface region may expand due to the presence of much H during treatment, and free H may penetrate into the deeper region of the bulk film through the modified and expanded network. The SIMS depth profile for the short-time D₂ plasma treatment (Fig. 5) shows that the incorporated amount of D increases with treatment time (which is the usual observation for this kind of SIMS experiment). Therefore, it is expected that the network expansion (or structural modification) due to hydrogenation is a continuous process as long as H (D) treatment continues. Consequently, a continuous increase of additional dangling bonds is expected during H treatment with time unlike the saturation of ΔN_s within a short time (< 1 s). Thus the fast saturation of ΔN_s cannot be the result of the network expansion during H treatment. Rather, the macroscopic network modification is the result of the db creation, termination, and annihilation due to in-diffusion of H.

In order to correlate our present *in situ* ESR results with those of earlier reports, we carried out the D₂ plasma treatment for a short time (for 10, 100, and 1000 s) on *a*-Si:H films at room temperature and studied the SIMS depth profiles *ex situ*. The following important information was found from the SIMS depth profile study.

(i) The number of incorporated H (D) ($> 10^{20} \text{ cm}^{-3}$ for 10 s of D₂ treatment) at the surface region is higher than the observed additional dangling bonds ($< 10^{19} \text{ cm}^{-3}$) created by H (D) treatment at the temperatures in the present study. In fact, the creation of db's by H is a competitive process between the creation, termination, and annihilation of the dangling bonds (as discussed in Sec. IV). So, effectively the number of dangling bonds created by H can be much lower than the incorporated amount of H.

(ii) A small amount of H ($< 10^{18} \text{ cm}^{-3}$), however, may diffuse into the bulk region (~ 100 nm) and create sufficient dangling bonds ($\sim 10^{17} \text{ cm}^{-3}$) to be detected in ESR. Figure 3 shows that the increase of additional db from 50 to 100 nm is $\sim 10^{12} \text{ cm}^{-2}$.

Therefore, the conjecture regarding fast saturation of ΔN_s is that, when H treatment starts on an as-deposited *a*-Si:H film (which has a low dangling-bond density), H diffuses very fast and creates additional dangling bonds that have a particular spatial distribution (i.e., exponential decrease from the film surface). In this case, perhaps almost each H atom creates a dangling bond. After the creation of dangling bonds within a very short time (< 1 s), the film contains a large amount of dangling bonds near the surface. Then the H diffusion will be impeded by the increased trapping probability at the dangling bonds in the vicinity of the surface. Thus such a free H diffusion process is self-limiting and reduces with treatment time (as estimated from Fig. 5). The steady state in the dangling-bond creation might occur due to either or both of the following two reasons.

(i) A small amount of H may have a high diffusion coefficient even for the films with high surface dangling bonds and permeate into the deeper region of *a*-Si:H films. Those small amounts of hydrogen ($< 10^{18} \text{ cm}^{-3}$) are perhaps sufficient to make a steady state between the annihilation term of reaction (5) and the creation term of reactions (2) and (3) to maintain the deep db distribution in the film [region II].

(ii) The H cannot diffuse in to the deeper region (~ 100 nm) after the creation of a large amount of dangling bonds at the film surface. However, the dangling bonds that are created in the deeper region at the initial stage (< 1 s) take a long time (much longer than our treatment time of 3 min) at our experimental temperature range to be annihilated or terminated by another hydrogen. Actually, we observed a slow decrease of dangling bonds for a longer H treatment time (~ 30 min) (Fig. 2 in Ref. 39). However, that decay does not confirm our above argument, since for longer treatment, there might be some etching of the film (which can reduce the number of dangling bonds as well). We believe that reason (i) is more probable than reason (ii) because Fig. 5 shows that D can diffuse into the film even at RT for the films deposited at RT (which are expected to contain a large number of db's).

The creation of metastable dangling bonds by breaking the weak or normal Si-Si bond is perhaps the first step for the modification of film structure due to H treatment on *a*-Si:H films. However, a small amount of H, which is below the detection limit for most of the practical cases and SIMS experiment, may have a high diffusion coefficient and permeate into the deeper region of *a*-Si:H films. Those small amounts of hydrogen ($\sim 10^{17} \text{ cm}^{-3}$) are sufficient to create a detectable amount of dangling bonds in ESR.

Therefore, considering all the above experimental results, we distinguish two different steps in which H interacts with the *a*-Si:H matrix. In step I, free H diffuses very fast ($D_f > 10^{-10} \text{ cm}^2 \text{ s}^{-1}$) into the film and creates db's during in-diffusion by reacting with the Si:H network according to processes (2)–(5). Such a high diffusion coefficient ($> 10^{-10} \text{ cm}^2 \text{ s}^{-1}$) of H is indeed reported in crystalline Si.⁴⁴ In step II, after the creation of db's within a short time < 1 s, the diffusion coefficient of H decreases due to the presence of a large number of db's. Then the effective diffusion coefficient of H (mixture of H in-diffusion and H diffusion by bond switching) might be less than $10^{-14} \text{ cm}^2 \text{ s}^{-1}$ through the modified network following the usual H diffusion processes explained elsewhere.^{31,33–35}

The fast diffusion of H and the creation of db's in *a*-Si:H films may have a correlation with the light-induced degradation processes in *a*-Si:H, since the motion of atomic H is assumed to be responsible for light-induced degradation in various models.^{20–23} In fact, Branz speculated such a high diffusion coefficient ($\sim 10^{-7} \text{ cm}^2 \text{ s}^{-1}$) of mobile H to explain the metastable degradation of *a*-Si:H films by pulsed illumination.⁴⁸

Regarding the interaction (more specifically, the trapping of H in weak or normal Si-Si bonds) of H in *a*-Si:H films, we observed that the dangling bonds are created at a shallower depth at higher treatment temperature (Fig. 6). Figure 4 confirmed that the db formation at a deeper place (film

depth of ~ 100 nm) is not due to any possible poor (void-rich) structure of the as-deposited film caused by lower T_d . Thus Fig. 6 and Eq. (11) imply that the trapping probability of free H (in other words, the reaction rate between H and the Si-Si network) increases with the increase of treatment temperature. The increase of rate constants for the db creation reactions at higher T_p result in the higher trapping density of free H and the formation of db closer to the film surface. The process thereby shortens the Δn_s distribution at higher temperatures. Also, the values of ΔN_s will be higher at the near-surface region (region I) at higher T_p . However, our present ESR signal-to-noise ratio for a small film thickness (~ 10 nm) is not enough to discuss the rate of initial increase of ΔN_s .

The difference of activation energies of db creation rate and the free H diffusion coefficient ($\Delta E_k - \Delta E_D$) is estimated to be 0.4 eV (inset of Fig. 6). The value of the activation energy for free H diffusion (ΔE_D) can be written as

$$\Delta E_D = kT \ln \left(\frac{D_0}{D_f} \right), \quad (12)$$

where k and D_0 are the Boltzmann constant and the diffusion prefactor, respectively. Considering the theoretical value of D_0 ($\sim 10^{-3} \text{ cm}^2 \text{ s}^{-1}$) (Ref. 29) and D_f of greater than $10^{-10} \text{ cm}^2 \text{ s}^{-1}$, the value of ΔE_D appears to be less than 0.5 eV. Thus the activation energy of free H diffusion is much less than the activation energy (~ 1.5 eV) for the layer diffusion of H observed by Carlson *et al.*³² and the activation energy (~ 0.8 eV) for the plasma in-diffusion of H observed by Beyer *et al.*³⁴ The relatively high activation energy and low diffusion coefficient observed by Beyer *et al.*³⁴ and by Jackson *et al.*³³ for the plasma in-diffusion of H by SIMS could be due to the combined effect of the free H diffusion and the layer diffusion (possibly through a bond-switching process). For the case of long-time (2 h) D_2 plasma treatment at greater than 200 °C, the contribution of the bonded D diffusion (similar to the layer diffusion) might be significant. In fact, that combined effect of two kinds of H diffusion (namely, the diffusion of free H and the diffusion of bonded H) may also explain the reported substantial variation of the coefficient and activation energy for H plasma in-diffusion in various types and duration of measurements (Table I). A low activation barrier of free H diffusion is, however, estimated from theoretical calculation and speculated from the D tracer diffusion by Branz.⁴⁸ It may also be pointed out that the usual Meyer-Neldel rule for the H diffusion coefficient and activation energy observed for the *a*-Si:H films³¹ deviates significantly for such a case of free H diffusion. This essen-

tially means that the diffusion mechanism for free H is perhaps different from the diffusion of H usually reported in the literature.

Considering the activated type of free H diffusion and $\Delta E_D < 0.5$ eV, we estimate that the activation energy for the db creation rate is within 0.4 to 0.9 eV. Lee *et al.* estimated the activation energy of less than 0.6 eV for the db creation in *a*-Si:H films from ESR measurements.⁵¹ The formation energy of 0.5–0.7 eV for Si db's in *a*-Si:H films was estimated from theoretical calculations by several authors.^{52–54} Therefore, the range of ΔE_k values ($0.4 \text{ eV} < \Delta E_k < 0.9 \text{ eV}$) estimated in this study is in reasonable agreement with the reported values of the formation energy of Si db's in *a*-Si:H films.

VI. CONCLUSION

In conclusion, we observed an unusually high diffusion coefficient ($D_f > 10^{-10} \text{ cm}^2 \text{ s}^{-1}$) of free atomic H in *a*-Si:H films during H treatment. The activation energy for such free H diffusion coefficient is less than 0.5 eV, which gives an estimate for the db creation energy of 0.4–0.9 eV. At the very initial stage (< 1 s), the fast diffusion of H results in additional db's that are spatially distributed in the bulk (~ 100 nm) of *a*-Si:H films. Such a fast diffusion of free H is a self-limiting process as db's created near the surface (in less than 1 s) act as trapping centers of the impinging H. Consequently, the effective diffusion coefficient of H reduces drastically ($D_{\text{eff}} < 10^{-14} \text{ cm}^2 \text{ s}^{-1}$) for longer treatment. The usual long-time D_2 plasma treatment and subsequent SIMS depth profile study give an estimate of the resultant diffusion coefficient for free H and bonded H. Thus the diffusion coefficient of H for plasma in-diffusion reported in the literature appears to be less than the free H diffusion coefficient but more than the H-layer diffusion coefficient. The depth of the db distribution due to the fast diffusion of H reduces with an increase of treatment temperature. Therefore it is suggested that the activation energy for a db creation is higher than the activation energy for a free H diffusion coefficient. The activated type of rate constant for the creation of db's determines the spatial distribution of db's.

ACKNOWLEDGMENTS

The authors are grateful to Professor K. Tanaka, Dr. S. D. Baranovskii, Dr. John Robertson, and Dr. W. Beyer for their encouragement and valuable comments on the paper. The work, which is partly supported by NEDO, was performed in the Joint Research Center for Atom Technology (JRCAT) under the joint research agreement between the National Institute for Advanced Interdisciplinary Research (NAIR) and the Angstrom Technology Partnership (ATP).

*Email address: ukdas@hotmail.com

¹J. I. Pankove, D. E. Carlson, J. E. Berkheiser, and R. O. Wance, *Phys. Rev. Lett.* **51**, 2224 (1983).

²N. M. Johnson, C. Herring, and D. J. Chadi, *Phys. Rev. Lett.* **56**, 769 (1986).

³S. J. Pearton, J. W. Corbett, and T. S. Shi, *Appl. Phys. A: Solids Surf.* **43**, 153 (1987), and references therein.

⁴J. W. Lyding, K. Hess, and I. C. Kizilyalli, *Appl. Phys. Lett.* **68**,

2526 (1996).

⁵P. J. Chen and R. M. Wallace, *Mater. Res. Soc. Symp. Proc.* **513**, 325 (1998).

⁶C. H. Seager and D. S. Ginley, *Appl. Phys. Lett.* **34**, 337 (1979).

⁷W. E. Spear and P. G. Lecomber, *J. Non-Cryst. Solids* **8–10**, 727 (1972).

⁸W. Beyer and J. Stuke, in *Amorphous and Liquid Semiconductors*, edited by J. Stuke and W. Bernig (Taylor and Francis,

- London, 1974) p. 245.
- ⁹W. E. Spear and P. G. Lecomber, *Solid State Commun.* **17**, 1193 (1975).
- ¹⁰S. Yamasaki, in *Glow Discharge Hydrogenated Amorphous Silicon*, edited by K. Tanaka (Kluwer, Boston, 1989), Chap. 4.
- ¹¹J. R. Abelson, *Appl. Phys. A: Solids Surf.* **56**, 493 (1993).
- ¹²U. K. Das, J. K. Rath, D. L. Williamson, and P. Chaudhuri, *Jpn. J. Appl. Phys.*, Part 1 **39**, 2530 (2000).
- ¹³I. Kaiser, N. H. Nickel, W. Fuhs, and W. Pilz, *Phys. Rev. B* **58**, R1718 (1998).
- ¹⁴R. A. Street, *Phys. Rev. B* **43**, 2454 (1991).
- ¹⁵K. Tanaka and A. Matsuda, *Mater. Sci. Rep.* **2**, 139 (1987).
- ¹⁶I. Shimizu, *J. Non-Cryst. Solids* **114**, 145 (1989).
- ¹⁷H. Shirai, D. Das, J. Hanna, and I. Shimizu, *Appl. Phys. Lett.* **59**, 1096 (1991).
- ¹⁸N. M. Johnson, C. E. Nebel, P. V. Santos, W. B. Jackson, R. A. Street, K. S. Stevens, and J. Walker, *Appl. Phys. Lett.* **59**, 1443 (1991).
- ¹⁹W. Futako, K. Yoshino, C. M. Fortmann, and I. Shimizu, *J. Appl. Phys.* **85**, 812 (1999).
- ²⁰M. Stutzmann, W. B. Jackson, and C. C. Tsai, *Appl. Phys. Lett.* **45**, 1075 (1984).
- ²¹C. Godet and P. Roca i Cabarrocas, *J. Appl. Phys.* **80**, 97 (1996).
- ²²R. Biswas, Q. Li, B. C. Pan, and Y. Yoon, *Phys. Rev. B* **57**, 2253 (1998).
- ²³H. M. Branz, *Phys. Rev. B* **59**, 5498 (1999).
- ²⁴J. B. Boyce and S. E. Ready, *Physica B* **170**, 305 (1991).
- ²⁵M. H. Brodsky, M. Cardona, and J. J. Cuomo, *Phys. Rev. B* **16**, 3556 (1977).
- ²⁶J. C. Knights, G. Lucovsky, and R. J. Nemanich, *Philos. Mag. B* **37**, 469 (1978).
- ²⁷A. A. Langford, M. L. Fleet, B. P. Nelson, W. A. Langford, and N. Maley, *Phys. Rev. B* **45**, 13 367 (1992).
- ²⁸C.-M. Chiang, S. M. Gates, S. S. Lee, M. Kong, and S. F. Bent, *J. Phys. Chem. B* **101**, 9537 (1997).
- ²⁹H. Fritzsche, M. Tanielian, C. C. Tsai, and P. J. Gaczi, *J. Appl. Phys.* **50**, 3366 (1979).
- ³⁰W. Beyer and H. Wagner, *J. Phys. (Paris), Colloq.* **42**, C4-773 (1981).
- ³¹W. Beyer, *Semiconductors and Semimetals* Vol. 61 (Academic, Orlando, 1999), p. 165.
- ³²D. E. Carlson and C. W. Magee, *Appl. Phys. Lett.* **33**, 81 (1978).
- ³³W. B. Jackson and C. C. Tsai, *Phys. Rev. B* **45**, 6564 (1992).
- ³⁴W. Beyer and U. Zastrow, in *Amorphous Silicon Technology—1996*, edited by M. Hock, E. A. Schiff, S. Wagner, R. Schropp, and A. Matsuda, MRS Symposia Proc. No. 420 (Materials Research Society, Pittsburgh, 1996), p. 497.
- ³⁵I. An, Y. M. Li, C. R. Wronski, and R. W. Collins, *Phys. Rev. B* **48**, 4464 (1993).
- ³⁶A. von Keudell and J. R. Abelson, *J. Appl. Phys.* **84**, 489 (1998).
- ³⁷S. Yamasaki, T. Umeda, J. Isoya, and K. Tanaka, *Appl. Phys. Lett.* **70**, 1137 (1997).
- ³⁸S. Yamasaki, T. Umeda, J. Isoya, and K. Tanaka, *J. Non-Cryst. Solids* **227–230**, 83 (1998).
- ³⁹S. Yamasaki, C. Malten, T. Umeda, J. Isoya, and K. Tanaka, in *Microcrystalline and Nanocrystalline Semiconductors—1998*, edited by M. J. Sailor *et al.*, MRS Symposia No. 536 (Materials Research Society, Pittsburgh, 1999), p. 463.
- ⁴⁰S. Yamasaki, U. K. Das, T. Umeda, J. Isoya, and K. Tanaka, *J. Non-Cryst. Solids* **266–269**, 529 (2000).
- ⁴¹U. K. Das, T. Yasuda, and S. Yamasaki, *Phys. Rev. Lett.* **85**, 2324 (2000).
- ⁴²T. Umeda, S. Yamasaki, J. Isoya, and K. Tanaka, *Phys. Rev. B* **59**, 4849 (1999).
- ⁴³J. Robertson, *J. Appl. Phys.* **87**, 2608 (2000).
- ⁴⁴A. Van Wieringen and N. Warmoltz, *Physica (Amsterdam)* **22**, 849 (1956).
- ⁴⁵J. Shinar, R. Shinar, S. Mitra, and J.-Y. Kim, *Phys. Rev. Lett.* **62**, 2001 (1989).
- ⁴⁶W. Beyer, *Physica B* **170**, 105 (1991).
- ⁴⁷B. Abeles, L. Yang, D. Leta, and C. Majkrzak, *J. Non-Cryst. Solids* **97&98**, 353 (1987).
- ⁴⁸H. M. Branz, *Phys. Rev. B* **60**, 7725 (1999).
- ⁴⁹M. Nakamura, T. Ohno, K. Miyata, N. Konishi, and T. Suzuki, *J. Appl. Phys.* **65**, 3061 (1989).
- ⁵⁰P. V. Santos and W. B. Jackson, *Phys. Rev. B* **46**, 4595 (1992).
- ⁵¹C. Lee, W. D. Ohlsen, and P. C. Taylor, *Phys. Rev. B* **36**, 2965 (1987).
- ⁵²Y. Bar-Yam, D. Adler, and J. D. Joannopoulos, *Phys. Rev. Lett.* **57**, 467 (1986).
- ⁵³Z. E. Smith and S. Wagner, *Phys. Rev. Lett.* **59**, 688 (1987).
- ⁵⁴P. C. Kelires and J. Tersoff, *Phys. Rev. Lett.* **61**, 562 (1988).